Frequency Control of Island VSC-HVDC Links Operating in Parallel With AC Interconnectors and Onsite Generation

Sotirios I. Nanou, *Member, IEEE*, and Stavros A. Papathanassiou, *Senior Member, IEEE*

***Abstract*—The main scope of this paper is to propose a suitable frequency control scheme for high-voltage dc-links (HVDC) based on voltage source converters (VSCs), operating in island systems with on-site conventional generation and external ac interconnectors. The proposed droop-type and inertia emulator is built upon the power synchronization control (PSC) concept, where grid synchronization is achieved without the need of a dedicated synchronization unit. The dynamics of the proposed PSC-based scheme are assessed both in frequency and time domain, utilizing a realistic study-case system, which corresponds to the current planning for the interconnection of Crete to the Greek mainland system, involving ac and dc interconnectors operating in parallel with conventional local thermal units. To demonstrate the benefits offered by the proposed controller in the context of frequency response, a detailed average value model is developed for the VSC-HVDC link in MATLAB/Simulink, where severe contingencies are simulated, such as the sudden loss of the external ac interconnector or local generation, leading from mainland grid-connected to islanded operation.**

***Index Terms*—High voltage dc transmission, frequency response, power synchronization control, inertia emulation, voltage source converter.**

I. Introduction

THE electrical interconnection of the Aegean Sea islands to the Greek mainland has been the subject of numerous feasibility studies so far, e.g. [1]–[3]. The latest ten-year network development plan of the Independent Power Transmission Operator (IPTO) foresees the interconnection of Crete to the Greek mainland system with ac interconnectors and high voltage dc links based on voltage source converters (VSC-HVDC), operating in parallel, whereas the need for maintaining local thermal generation is currently under investigation, to ensure reserves for N-1 contingencies [3]–[5].

For island interconnection projects with the aforementioned characteristics, a flexible control scheme is needed for the island VSC, capable of supporting both grid-connected (ac-link in operation) and islanded passive network operation (ac link and local generation not active), while ensuring a seamless transition from one condition to the other, without the need to perform control mode changes in real-time, that might jeopardize continuity of supply. Comparing the state-of-the-art control techniques proposed so far for VSC-HVDC systems operating in weak ac systems [6]–[16], there is a group of control variants which do not require a dedicated synchronization unit in order to achieve grid synchronization, thus overcoming performance limitations of the conventional synchronous reference frame (SRF) vector-current controller in weak ac systems or in complete absence of an external voltage source [9]. More specifically, in [11] and [12] suitable control loops are proposed in order to model the swing equation of a synchronous generator, thus the angular frequency reference of the converter output voltage is determined by a virtual generator control loop. However, the control scheme proposed in [11] does not cater for over-current situations which could result from grid faults, whereas in [12] a vector current controller is also included in order to prevent over-current blocking of the VSC during grid faults. Another control variant with similar high level characteristics is the power synchronization control (PSC) concept, first proposed in [9] for HVDC converters, in which the phase angle of the converter output voltage is directly determined by a simple integrator instead of the swing equation, as in the aforementioned control schemes, thus not addressing the challenge of providing synthetic inertia response. The PSC scheme includes also a suitable current controller in order to handle over-current situations and provide adequate damping to the PSC loop, thus constituting a good candidate for real world VSC-HVDC interconnection projects.

Even though droop-type and inertia emulation control (INEC) schemes are already identified in the literature for VSCs employing conventional vector-current control [17]–[22], the implementation of similar frequency control techniques for VSCs employing PSC is still under investigation, since the operating frequency of the VSC is not determined by means of an external frequency estimation unit, but it is governed by an active power control loop, whose dynamic characteristics establish the anticipated frequency response.

In this paper, an enhanced PSC scheme is introduced for island VSC-HVDC links, which provides both droop-type and inertia response by perturbing the operating frequency of the

Manuscript received February 10, 2017; revised May 21, 2017; accepted June 20, 2017. Date of publication July 3, 2017; date of current version January 22, 2018. Paper no. TPWRD-00222-2017. *(Corresponding Author: Sotirios I. Nanou.)*

The authors are with the School of Electrical and Computer Engineering, National Technical University of Athens, Zografou 15780, Greece (e-mail: sotnanou@gmail.com; st@power.ece.ntua.gr).

Color versions of one or more of the figures in this paper are available online at http://ieeexplore.ieee.org.

Digital Object Identifier 10.1109/TPWRD.2017.2722498

VSC, thus satisfying all related requirements of the latest grid codes for HVDC systems [23]. Specifically, apart from the conventional droop-type controller, which comprises the core block of the PSC loop under study, a suitable INEC scheme is also included, preventing large frequency excursions following severe contingencies, such as the loss of the ac interconnector. The dynamic characteristics of the proposed PSC-based scheme are analyzed in the frequency domain via a suitable small-signal model. Then, the ability of the VSC-HVDC link to perform effective frequency control in islanded mode, avoiding large frequency excursions during severe disturbances, is examined through time-domain simulations, utilizing a detailed average value model for the VSC-HVDC link.

The paper is organized as follows. The study-case island system is presented in Section II. The dynamics of the proposed PSC-based frequency control concept are investigated in Section III and the detailed control scheme for the VSC-HVDC link is outlined in Section IV. The transient response of the island system following severe contingencies is demonstrated in Section V, through time-domain simulations. The main conclusions are summarized in Section VI, whereas basic system parameter values and controller settings are provided in the Appendix.

II. Study-Case System

The generic layout of the island system considered in this paper is depicted in Fig. 1. The VSC-HVDC link comprises the mainland VSC, the island VSC and two ±320 kV, 300 km long submarine cables. The active power transfer capability of the dc link is assumed 1000 MW. The island grid is represented in Fig. 1 by a single bus system, to which the ac & dc interconnectors and the local load are connected. The mainland grid is represented by its Thevenin equivalent. To guarantee secure operation without load shedding following severe contingencies, local generating units (typically internal combustion engines (ICE) or gas turbines) may be committed to provide spinning reserves during high load conditions, as discussed in more detail in [4], [5]. For this purpose, a conventional local power station, comprising an aggregate 200 MW ICE generator, is also shown in Fig. 1. The ICE unit model incorporates a Woodward type speed governor and a standard automatic voltage regulator [24].

To simplify converter modeling and reduce computational burden, an average value model is developed for the mainland and island VSCs, based on modeling techniques available in the literature for state-of-the art modular multilevel converters (MMC) [25]–[29]. Due to the non-negligible capacitance of the HVDC cables, the distributed parameter line model is employed, using the parameter values given in Table II of the Appendix.

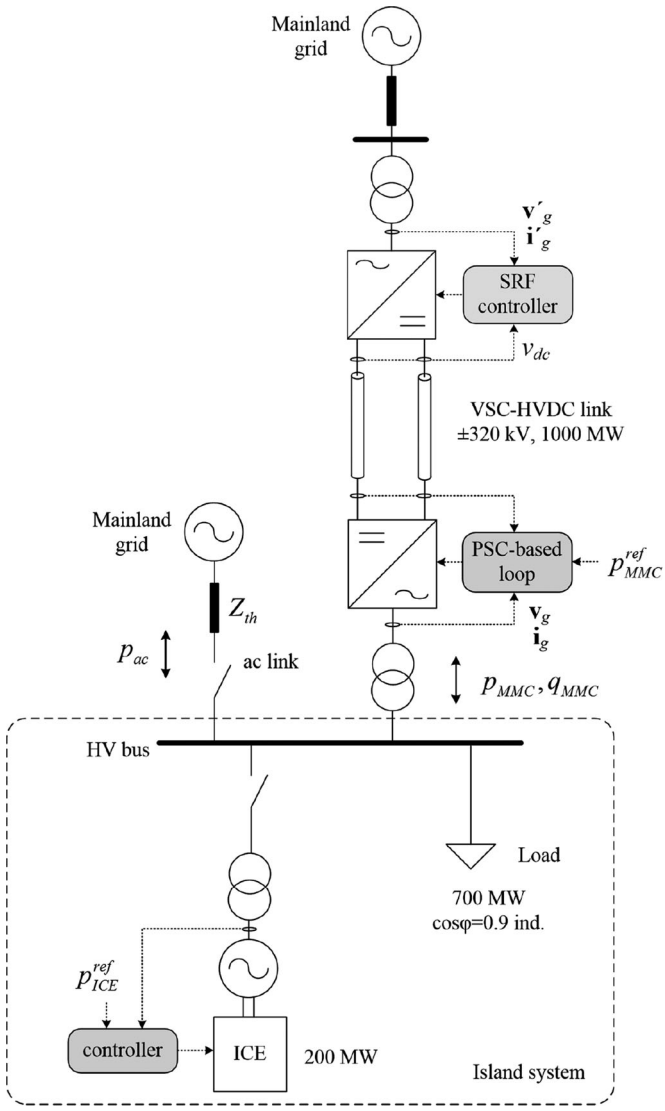

Fig. 1. Generic layout of the study-case island system comprising mixed ac & dc interconnectors, local thermal units and local load.

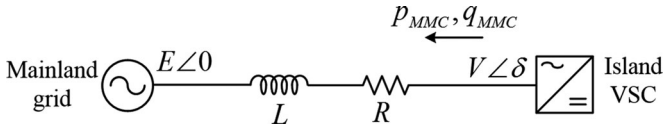

Fig. 2. Conceptual interconnection between island VSC and mainland grid (via the ac interconnector) for stability analysis of the proposed PSC-based VSC control scheme.

III. PSC-Based Frequency Control Scheme

So far, standard control schemes for grid-connected VSCs utilize a dedicated synchronization unit in order for the controller to operate in the SRF [6]–[8]. However, alternative controllers are emerging in the literature [9]–[12], where the operating frequency of the VSC is governed by an active power control loop, emulating the natural synchronization process among synchronous machines. In the following, the PSC control concept is adopted and tailored to island interconnection applications.

Fig. 2 shows a simplified HVDC-VSC grid connection, where the inductor L and resistor R represent the equivalent network impedance between the island VSC and the mainland grid via the ac interconnector. The small-signal model of the proposed PSC-based scheme is illustrated in block diagram form in Fig. 3, following the approach of [9]. $J_{P\delta}(s)$ is the ac system transfer

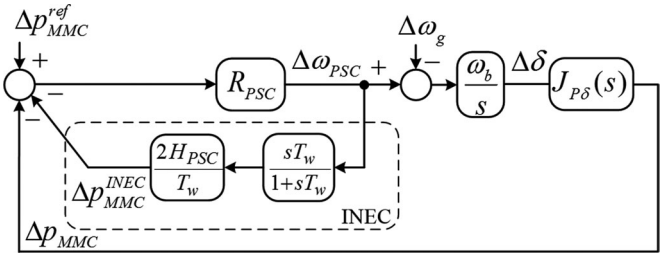

Fig. 3. Proposed PSC-based scheme in block diagram form.

function from $\Delta\delta$ to Δp_{MMC}, which is given by [9]:

$$J_{P\delta} = \frac{a_0 s^2 + a_1 s + a_2}{(sL + R + H_{HP}(s))^2 + (\omega_0 L)^2} \tag{1}$$

where

$$\begin{aligned} a_0 &= L(E_0 V_0 \cos\delta_0 - V_0^2)/\omega_0 \\ a_1 &= (R + H_{HP}(s))(E_0 V_0 \cos\delta_0 - V_0^2)/\omega_0 \\ a_2 &= \omega_0 L E_0 V_0 \cos\delta_0 - (R + H_{HP}(s)) E_0 V_0 \sin\delta_0 \end{aligned} \tag{2}$$

As discussed in Section IV, $H_{HP}(s)$ is a high-pass filter imposed on the measured VSC output current to increase damping in case of small values of *R,* described by:

$$H_{HP}(s) = \frac{k_v s}{s + \alpha_v} \tag{3}$$

The proposed VSC control scheme is built on the PSC variant presented in [30], which relies on a simple proportional compensator (gain R_{PSC} in Fig. 3) to effect changes in the phase angle δ in order to meet the active power reference p^{ref}_{MMC}. As explained in [30], this compensator constitutes a virtual frequency droop controller, since steady-state active power regulation errors are induced in the presence of frequency deviations. In this paper, the PSC scheme is further augmented, by including the additional INEC loop depicted in Fig. 3, which introduces synthetic inertia response characteristics.

The proposed scheme utilizes the controlled operating frequency $\Delta\omega_{PSC}$, in order to estimate the rate of change of frequency (ROCOF) on the island, by means of a typical washout filter. Then, an active power deviation signal Δp^{INEC}_{MMC} is superposed on the reference Δp^{ref}_{MMC}, proportional to the equivalent inertia constant H_{PSC} of the island VSC. Therefore, the active power controller depicted in Fig. 3 constitutes a combined droop-type and inertia emulator, without any need for an external frequency estimation unit.

To assess the effect of the INEC gain H_{PSC} on the PSC dynamics, the open-loop transfer function $G_{PSC}(s)$ in the frequency-domain is used:

$$G_{PSC}(s) = \frac{R_{PSC}}{1 + R_{PSC}\frac{2sH_{PSC}}{1+sT_w}} \frac{\omega_b}{s} J_{P\delta}(s) \tag{4}$$

The Bode diagram of $G_{PSC}(s)$ is plotted in Fig. 4 for different values of H_{PSC}, assuming a droop gain $R_{PSC} = 5\%$, typical for conventional generators. Higher H_{PSC} values tend to reduce

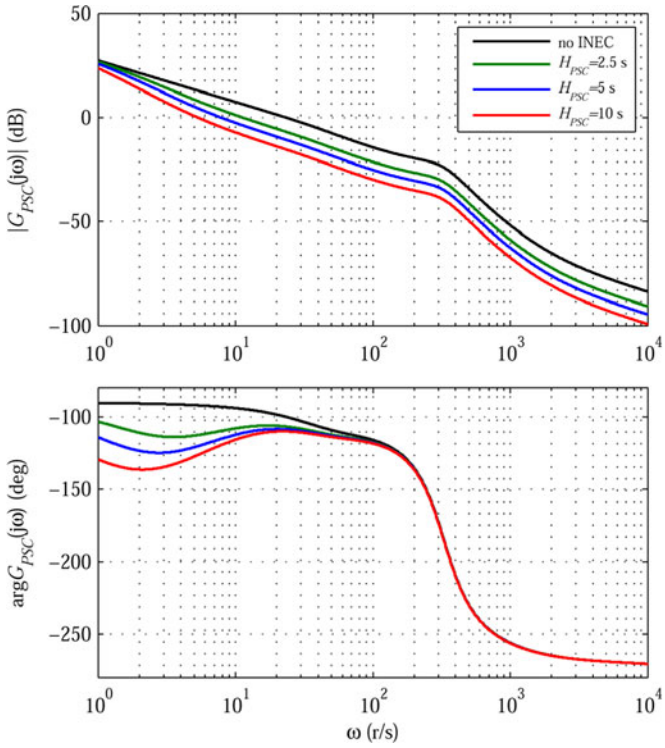

Fig. 4. Bode diagram of the open-loop transfer function $G_{PSC}(s)$ for different virtual inertia gains H_{PSC} ($R_{PSC} = 5\%$, $L = 0.5$ p.u., $R = 0.01$ p.u., $k_v = 0.2$, $\alpha_v = 40$ r/ s, $T_w = 0.2$ s).

the response time of the system, as expected, due to the inertia emulation mechanism. However, the impact of the INEC term on system stability is not affected solely by the gain H_{PSC}, but also by the time constant T_w of the washout filter shown in Fig. 3, based on which a ROCOF estimate is obtained. The effect of T_w is illustrated in the Bode plots of Fig. 5. Very low T_w values tend to reduce the phase margin of the system close to the stability limit ($-180°$), while excessive lag ($\sim$1 s) maintains satisfactory phase margin levels, but inevitably degrades the inertia response capability of the VSC. $T_w = 0.2$ s is selected in this work, as a good compromise between speed and stability.

IV. Proposed Control Scheme For the VSC-HVDC Link

A. Mainland MMC Controller

The overall control scheme employed for the mainland MMC is depicted in Fig. 6(a) [30], [31]. In normal operating conditions, the mainland MMC regulates the HVDC voltage v_{dc} via a proportional – integral (PI) compensator controlling the power exchange with the grid. For the inner control loop, a conventional SRF vector-current controller is employed to regulate the inverter output current, providing suitable modulation indices to the submodule controller of the actual MMC topology, as further explained in [30]; in this work, an equivalent average value model is utilized.

The synchronization unit depicted in Fig. 6(a) comprises a conventional phase locked loop (PLL) equipped with a positive sequence extraction unit based on Double Second Order Generalized Integrator (DSOGI) filters. This enables handling

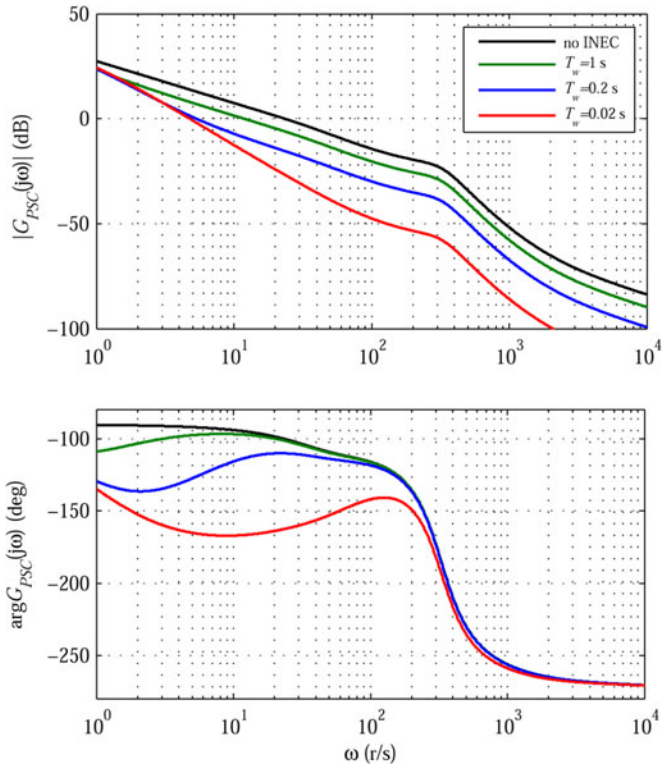

Fig. 5. Bode diagram of the open-loop transfer function $G_{\mathrm{PSC}}(s)$, for different T_{w} values of the washout filter ($R_{PSC} = 5\%$, $H_{PSC} = 5$ s, $L = 0.5$ p.u., $R = 0.01$ p.u., $k_v = 0.2$, $\alpha_v = 40$ r/ s).

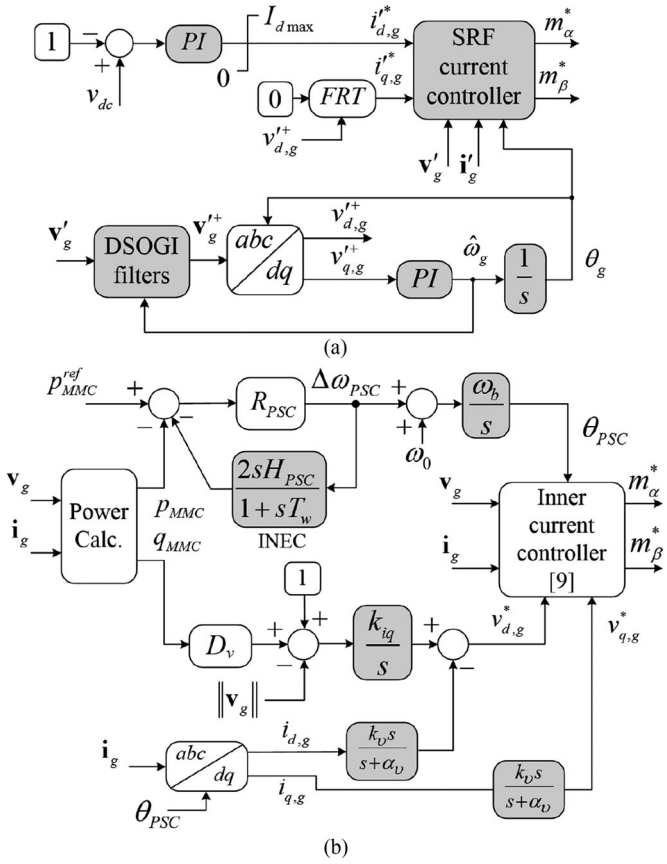

Fig. 6. Control structure of the VSC-HVDC link. (a) Mainland MMC control scheme, (b) Island MMC control scheme.

unbalanced grid conditions, as explained in detail in [31], as well as estimating the positive sequence component during voltage dips in order to regulate reactive current injection when entering Fault Ride-Through (FRT) mode.

B. Island MMC Controller

The island MMC controller, which is the primary focus in this work, is depicted in detail in Fig. 6(b). As explained in Section III, the dynamic behavior of a VSC employing PSC resembles an interconnected synchronous machine, since the transmitted active power varies directly by controlling the phase angle θ_{PSC} of the VSC output voltage phasor. In a similar manner, reactive power is controlled by adjusting the output voltage magnitude of the VSC, using a droop characteristic (gain D_v in Fig. 6(b)). The inner current control loop shown in Fig. 6(b) is only necessary in order to prevent VSC overcurrent in case of ac system faults, whereas a high-pass filter is applied to the measured *d-q* axis components in order to provide adequate damping to the PSC loop. The PSC-based scheme in Fig. 6(b) provides adjustable droop and inertia response, significant in islanded operation, by tuning gains R_{PSC} and H_{PSC} respectively.

In the presence of the external ac interconnector, island load variations are normally supplied by the ac link, due to the fixed operating frequency imposed on the island. Therefore, under normal conditions the island VSC operates in active power control mode, tracking the set-point p^{ref}_{MMC}, established by an external system, such as a controller monitoring power flows on the ac interconnector (essentially an Automatic Generation Control (AGC) functionality) or an economic dispatch module.

Following a fault/failure leading to the tripping of the ac link, the VSC should be able to transition from the aforementioned operating mode, either to grid-forming operation, in case of a passive island network, or to frequency-sensitive mode, participating in primary frequency control in parallel to conventional generation operating on the island. A central benefit of the proposed PSC-based control scheme depicted in Fig. 6(b) is that the island VSC is inherently capable of seamlessly transitioning from one operating mode to the other, without any control mode switching, as it will be further demonstrated in Section V.

V. Time-Domain Simulations

The objective of this section is to demonstrate the frequency response capabilities of the VSC-HVDC link utilizing the proposed PSC-based frequency control concept, as well as to verify the controller design performed in Section III. For this purpose, an extreme operating scenario is simulated, where the sudden loss of the ac link is followed by tripping of the local ICE generating unit (both simulated by successively opening the respective breakers in Fig. 1), signifying a transition from grid-connected to passive network operation. The analysis is performed under peak island load conditions, approximately

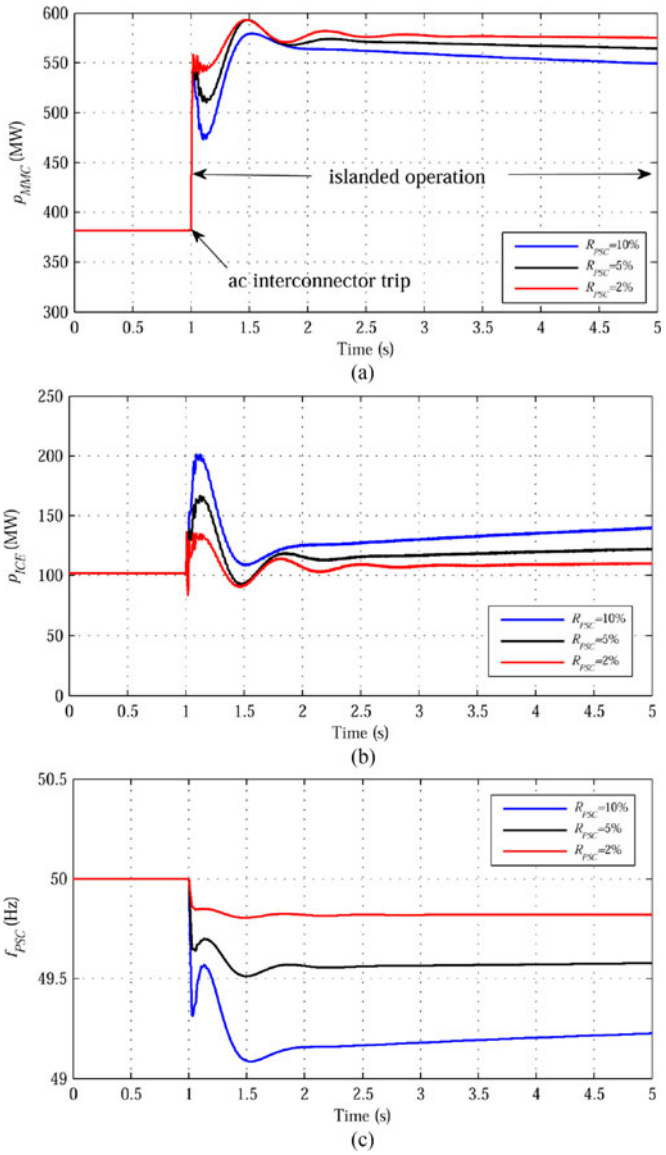

Fig. 7. Response following the loss of the external ac interconnector, for different R_{PSC} gains. (a) Active output power of the island MMC, (b) ICE generator power, (c) operating frequency of the island MMC.

700 MW, when all interconnections and generating units operate in parallel. Prior to the disturbance, the ICE unit is operating at a low output power (50% of rated), while the scheduled active power imported via the ac link is regulated to 200 MW.

For the simulations conducted in this Section, the SimPowerSytems Toolbox of Matlab/Simulink has been used, with the Electromagnetic Transient (EMT) simulation method [32]. All high-frequency components related to the switching of power converters are neglected and suitable average value MMC models are employed, based on typical parameter values (in p.u.) reported in the literature [25]–[29]. System parameters and controller settings are given in the Appendix.

A. Response Following the Loss of the External AC Link Without INEC

In Fig. 7, the response of the VSC-HVDC link and the local ICE station is presented, first assuming that the ac connection

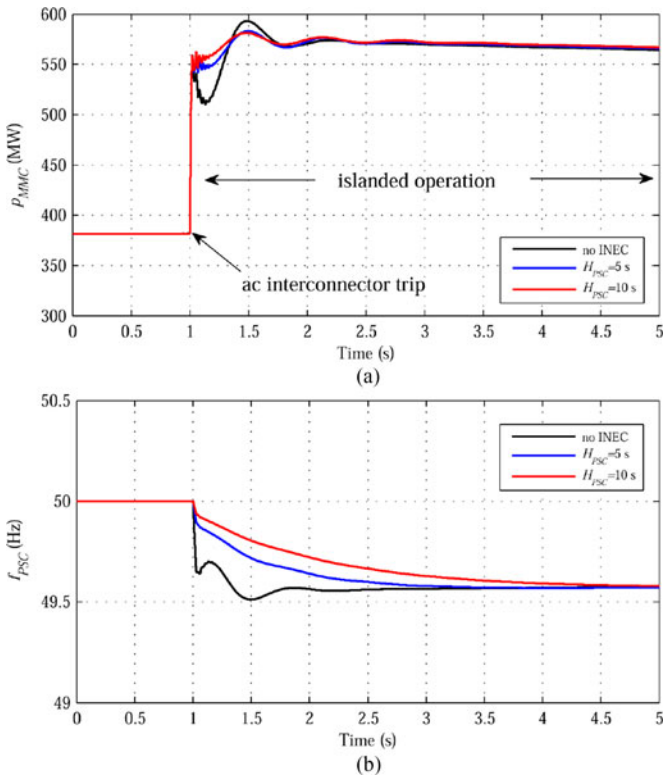

Fig. 8. Response of the island MMC following a loss of the external ac interconnection, for different virtual inertia H_{PSC} values. (a) Active output power, (b) operating frequency.

to the mainland grid trips at 1 s. To demonstrate the inherent capability of the island VSC employing the proposed PSC loop to operate in power sharing mode with the local ICE units, three different R_{PSC} gains are tested, while the INEC path remains inactive. Upon islanding at $t = 1$ s, the local frequency experiences a drop depending on the effective droop gains of the island VSC and the local ICE station, while the transient response of the MMC active output power is fast and well-damped in all cases. Low droop R_{PSC} values contain effectively the excursions of the local frequency and thus the active power transients of the local ICE unit in Fig. 7(b). Nevertheless, from Fig. 7(c) it is clear that very high ROCOF values can appear right after the disturbance, an issue which is further analyzed in the following section.

B. Response Following the Loss of the External AC Link With the Proposed INEC Scheme Integrated in the PSC Loop

In Figs. 8 and 9, the same disturbance as in Fig. 7 is simulated, now with the inertia controller (INEC) activated for the island MMC. A moderate and a high virtual inertia constant H_{PSC} are tested, with a PSC droop gain $R_{PSC} = 5\%$.

If no INEC is applied, as in the previous section, the abrupt frequency drop observed in both diagrams of Figs. 8(b) and 9(b), leads to short-term but high ROCOF values (>1 Hz/s), obtained either with a 500 ms or a 100 ms rolling measurement window. Hence, although the PSC loop can contain the maximum frequency excursion, it is still unable to maintain ROCOF values at low levels, due to the limited inertia of the islanded system.

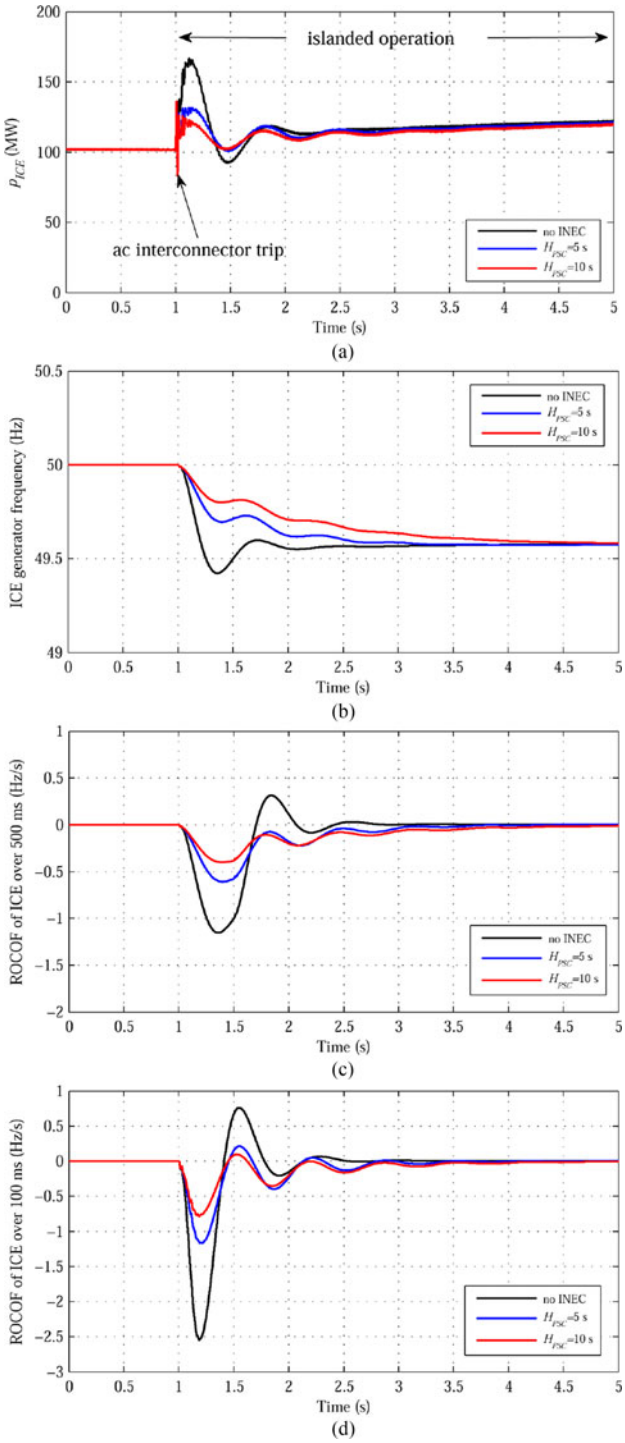

Fig. 9. Response of the local ICE station following the loss of the external ac link, for different virtual inertia H_{PSC} values of the island MMC controller. (a) ICE generator power, (b) ICE generator frequency, (c) ROCOF evaluated through a 500 ms rolling measurement window, (d) ROCOF evaluated through a 100 ms rolling measurement window.

This raises concern regarding the security of the island system following severe contingencies, as high ROCOF values may trigger the protection of generating units (typical settings for distributed generation lie in the range of 0.5-1 Hz/s [33], [34]) or lead to load shedding, if a ROCOF-sensitive scheme is implemented on the island. Furthermore, the even higher ROCOF

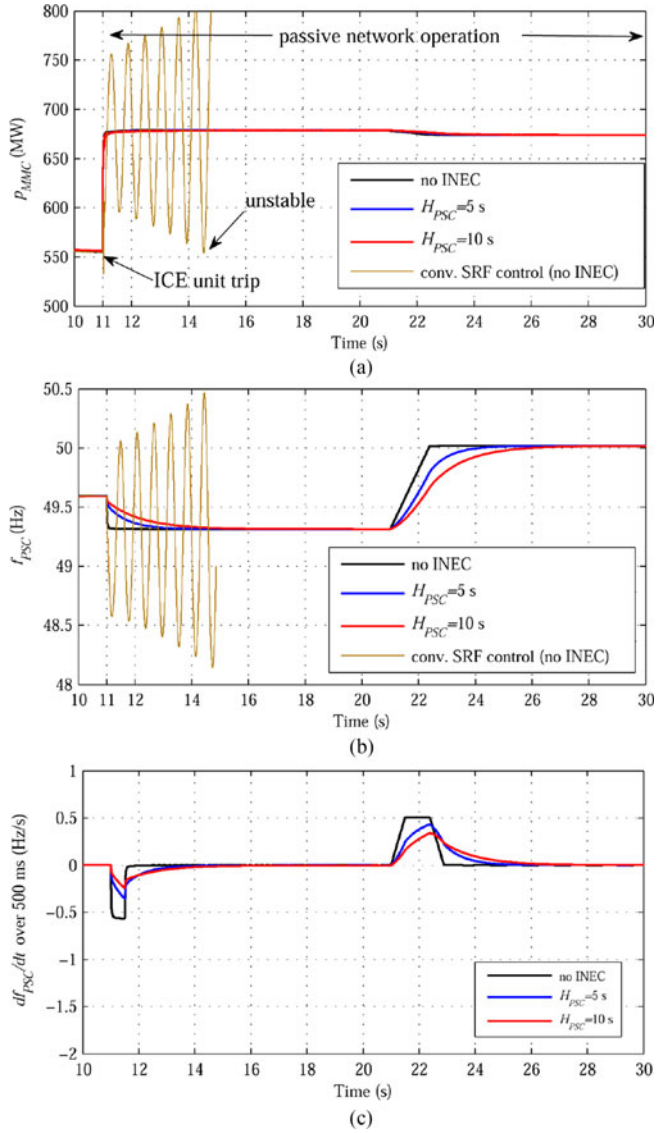

Fig. 10. Response of the island MMC following the loss of the local ICE unit at $t = 11$ s, while the system operates as in Fig. 8 after the ac interconnector trip, and subsequent restoration of frequency at $t = 21$ s, for different virtual inertia H_{PSC} values. (a) Active output power, (b) operating frequency, (c) ROCOF estimate over a 500 ms rolling measurement window.

values (>2 Hz/s) observed in Fig. 9(d) using a 100 ms window, are also questionable with regards to withstand capability of existing generation to high ROCOF values [35].

The positive impact of the proposed INEC scheme is illustrated in Figs. 8 and 9, for a typical and a relatively high H_{PSC} value (5 s and 10 s respectively). The inertia emulation limits instantaneous ROCOF to the level of 1 Hz/s and below, irrespective of the applied rolling measurement window, while the overall variation of the frequency on the island is much smoother and its maximum excursion reduced.

C. Response Following the Combined Loss of External AC Link and Local ICE Unit

The scenario simulated in Figs. 7–9 evolves further in Fig. 10, assuming that the local ICE unit trips 10 s after the loss of

the ac link (i.e. at $t = 11$ s), thus leading to passive network operation. The PSC scheme again succeeds in readjusting the active power p_{MMC} of the HVDC link, without unacceptable frequency excursions or high ROCOF values when the INEC regulation path is active. A noteworthy observation is that the island frequency can be restored back to its nominal value simply by increasing the active power set-point p^{ref}_{MMC} in Fig. 6(b), an action which does not affect the active power imported to the island by the HVDC link. This is simulated at $t = 21$ s in Fig. 10, assuming a ramp rate limit of 0.2 p.u./s for p^{ref}_{MMC}, in order to prevent high ROCOF values that could be induced by the controller response to step input changes.

To further support the advantages of the PSC-based approach when transitioning to passive network operation, additional simulation results are included in Fig. 10(a) and (b), employing the conventional SRF control of [6], [13] for the island VSC, utilizing a PLL unit for grid synchronization. It is evident that the conventional SRF controller would not be able to achieve a stable response, due to the inability of the PLL unit to maintain synchronism in the absence of an external voltage source (mainland ac network or local generating units).

VI. Conclusion

In this paper, an augmented PSC scheme was introduced for island VSC-HVDC links, to achieve droop-type and inertia frequency response solely via modulation of the operating frequency of the island VSC. Such functionality is essential in order to comply with the latest grid code requirements for HVDC systems, as well as to guarantee the dynamic security of the island system during severe N-1 contingencies. The frequency domain analysis illustrates that the combined droop and inertia control scheme proposed in this work does not compromise the stability of the PSC loop, provided that the washout filter of the INEC path is properly tuned.

Time-domain simulations were performed to assess the frequency response of the island system following severe N-1 contingency events, simulated by the sudden loss of the external ac interconnector, then followed by tripping of the local thermal station. It was shown that the island VSC seamlessly transitions from grid-connected to islanded operation, while the proposed INEC loop effectively contains frequency transients and induced ROCOF values.

Appendix

Parameter values and controller settings for the MMCs and the VSC-HVDC link of Fig. 1 are given in Tables I–IV.

TABLE I
MMC Parameter Values

Parameter	Value
MMC nominal active power	1000 MW
Nominal dc voltage	$\pm$320 kV
MMC rated current	1.95 kA
Equivalent dc capacitance of each MMC	315 μF
Arm inductance	60.3 mH

TABLE II
VSC-HVDC Link and Mainland System Parameter Values

Parameter	Value
Ac system nominal voltage	150 kV
Grid Thevenin impedance Z_{th}	$7.5\angle 80^{\circ}\Omega$
Transformer (TF) power rating	1200 MVA
Mainland TF voltage ratio	400/320 kV
Island TF voltage ratio	320/150 kV
TF leakage reactance	15%
HVDC cable resistance	0.011 Ω/km
HVDC cable inductance	2.62 mH/km
HVDC cable capacitance	0.2 μF/km

TABLE III
Mainland MMC Controller Parameter Values

Parameter	Value
PI controller of v_{dc}	$4.85 + 4.85/(0.09s)$
SRF PI current controller	$0.4 + 0.4/(0.005s)$
PI controller of $v^{l+}_{q,g}$	$80 + 80/(0.025s)$

TABLE IV
Island MMC Controller Parameter Values

Parameter	Value
PSC droop gain R_{PSC} (default value)	5% (adjustable)
INEC gain H_{PSC}	adjustable
Washout filter time constant T_w	0.2 s
Voltage droop gain D_v	10%
Voltage controller gain k_{iq}	5
High-pass filter gain k_v	0.2
High-pass filter parameter α_v	40 r/s

Acknowledgment

The postdoctoral research of Dr. Sotirios Nanou is performed in the framework of the Action "SUPPORTING POSTDOCTORAL RESEARCHERS" of the Operational Programme "Human Resources Development, Education and Life Long Learning", 2014–2020, implemented by IKY and co-financed by the European Social Fund and the Public Investments Programme.

References

[1] M. Papadopoulos, N. Boulaxis, M. Tsili, and S. Papathanassiou, "Increased wind energy exploitation via interconnection of Aegean island to the mainland grid," in *Proc. 19th Int. Conf. Elect. Distrib.*, Vienna, Austria, 2007, pp. 1–4.

[2] *System Development Study of Crete: Interconnection to the Mainland Grid – Extended Synopsis*. Athens, Greece: Hellenic TSO, Public Power Corporation, and Regulatory Authority for Energy, Apr. 2011.

[3] *Ten Year Network Development Plan 2017–2026*. Athens, Greece: Independent Power Transmission Operator, Mar. 2016.

[4] S. Nanou, M. Papadopoulos, and S. Papathanassiou, "Assessment of island interconnection projects via HVDC links of partial capacity: The case of Crete," in *Proc. Cigre Paris Session*, Aug. 2016, no. C1–202.

[5] M. Karystianos, Y. Kabouris, T. Koronides, and S. Sofroniou, "Operation of the electrical system of Crete in interconnection with the mainland Grid: A stability study," in *Proc. IREP Symp. Bulk Power Syst. Dyn. Control IX Optim. Security Control Emerg. Power Grid*, 2013, pp. 1–8.

[6] A. Yazdani and R. Iravani, *Voltage-Sourced Converters in Power Systems: Modeling, Control, and Applications*. New York, NY, USA: Wiley, 2010.
[7] W. Wang, A. Beddard, M. Barnes, and O. Marjanovic, "Analysis of active power control for VSC – HVDC," *IEEE Trans. Power Del.*, vol. 29, no. 4, pp. 1978–1988, Aug. 2014.
[8] A. Egea-Alvarez, S. Fekriasl, F. Hassan, and O. Gomis-Bellmunt, "Advanced vector control for voltage source converters connected to weak grids," *IEEE Trans. Power Syst.*, vol. 30, no. 6, pp. 3072–3081, Nov. 2015.
[9] L. Zhang, L. Harnefors, and H.-P. Nee, "Power-synchronization control of grid-connected voltage-source converters," *IEEE Trans. Power Syst.*, vol. 25, no. 2, pp. 809–820, May 2010.
[10] L. Zhang, L. Harnefors, and H.-P. Nee, "Modeling and control of VSC-HVDC links connected to island systems," *IEEE Trans. Power Syst.*, vol. 26, no. 2, pp. 783–793, May. 2011.
[11] Q.-C. Zhong and G. Weiss, "Synchronverters: Inverters that mimic synchronous generators," *IEEE Trans. Ind. Electron.*, vol. 58, no. 4, pp. 1259–1267, Apr. 2011.
[12] M. Guan, W. Pan, J. Zhang, Q. Hao, J. Cheng, and X. Zheng, "Synchronous generator emulation control strategy for voltage source converter (VSC) stations," *IEEE Trans. Power Syst.*, vol. 30, no. 6, pp. 3093–3101, Nov. 2015.
[13] A. L. Rocabert, F. Blaabjerg, and P. Rodriguez, "Control of power converters in AC microgrids," *IEEE Trans. Power Electron.*, vol. 27, no. 11, pp. 4734–4749, Nov. 2012.
[14] M. Guan and Z. Xu, "Modeling and control of a modular multilevel converter-based HVDC system under unbalanced grid conditions," *IEEE Trans. Power Electron.*, vol. 27, no. 2, pp. 4858–4867, Dec. 2012.
[15] Y. Li *et al.*, "Power compensation control for interconnection of weak power systems by VSC-HVDC," *IEEE Trans. Power Del.*, vol. 32, no. 4, pp. 1964–1974, Aug. 2017.
[16] M. Saeedifard and R. Iravani, "Dynamic performance of a modular multilevel back-to-back HVDC system," *IEEE Trans. Power Del.*, vol. 25, no. 4, pp. 2903–2912, Oct. 2010.
[17] L. M. Castro and E. Acha, "On the provision of frequency regulation in low inertia ac grids using HVDC systems," *IEEE Trans. Smart Grid*, vol. 7, no. 6, pp. 2680–2690, Nov. 2016.
[18] J. Zhu, C. D. Booth, G. P. Adam, A. J. Roscoe, and C. G. Bright, "Inertia emulation control strategy for VSC-HVDC transmission systems," *IEEE Trans. Power Syst.*, vol. 28, no. 2, pp. 1277–1287, May 2013.
[19] C. Du, E. Agneholm, and G. Olsson, "Use of VSC-HVDC for industrial systems having onsite generation with frequency control," *IEEE Trans. Power Del.*, vol. 23, no. 4, pp. 2233–2240, Oct. 2008.
[20] C. Du, E. Agneholm, and G. Olsson, "Comparison of different frequency controllers for a VSC-HVDC supplied system," *IEEE Trans. Power Del.*, vol. 23, no. 4, pp. 2224–2232, Oct. 2008.
[21] H. Liu and Z. Chen, "Contribution of VSC-HVDC to frequency regulation of power systems with offshore wind generation," *IEEE Trans. Energy Convers.*, vol. 30, no. 3, pp. 918–926, Sep. 2015.
[22] J. Renedo, A. Garcia-Cerrada, and L. Rouco, "Active power control strategies for transient stability enhancement of AC/DC grids with VSC-HVDC multi-terminal systems," *IEEE Trans. Power Syst.*, vol. 31, no. 6, pp. 4595–4604, Nov. 2016.
[23] Commission Regulation (EU) 2016/1447 on establishing a network code on requirements for grid connection of high voltage direct current systems and direct current-connected power park modules, 2016, O.J. L 241/1.
[24] S. V. Papaefthymiou, V. G. Lakiotis, I. D. Margaris, and S. A. Papathanassiou, "Dynamic analysis of island systems with wind-pumped-storage hybrid power stations," *Renew. Energy*, vol. 74, pp. 544–554, 2015.
[25] H. Saad *et al.*, "Dynamic averaged and simplified models for MMC-Based HVDC transmission systems," *IEEE Trans. Power Del.*, vol. 28, no. 3, pp. 1723–1730, Jul. 2013.
[26] J. Peralta, H. Saad, S. Dennetiere, J. Mahseian, and S. Nguefeu, "Detailed and averaged models for a 401-level MMC-HVDC system," *IEEE Trans. Power Del.*, vol. 27, no. 3, pp. 1501–1508, Jul. 2012.
[27] N.-T. Trinh, M. Zeller, K. Wuerflinger, and I. Erlich, "Generic model of MMC-VSC-HVDC for interaction study with AC power system," *IEEE Trans. Power Syst.*, vol. 31, no. 1, pp. 27–34, Jan. 2016.
[28] H. Yang, Y. Dong, W. Li, and X. He, "Average-Value model of modular multilevel converters considering capacitor voltage ripple," *IEEE Trans. Power Del.*, vol. 32, no. 2, pp. 723–732, Apr. 2017.
[29] Q. Song, W. Liu, X. Li, H. Rao, S. Xu, and L. Li, "A steady-state analysis method for a modular multilevel converter," *IEEE Trans. Power Electron.*, vol. 28, no. 8, pp. 3702–3713, Aug. 2013.
[30] S. I. Nanou and S. A. Papathanassiou, "Grid code compatibility of VSC-HVDC connected offshore wind turbines employing power synchronization control," *IEEE Trans. Power Syst.*, vol. 24, no. 6, pp. 1537–1546, Nov. 2016.
[31] S. Nanou and S. Papathanassiou, "Evaluation of a communication-based fault ride-through scheme for offshore wind farms connected through high-voltage DC links based on voltage source converter," *IET Renew. Power Gener.*, vol. 9, pp. 882–891, Nov. 2015.
[32] Hydro-Québec and The MathWorks, Inc., "SimPowerSystems™ User's Guide," Hydro-Québec and The MathWorks, Inc., Natick, MA, USA, 2010.
[33] J. O'Sullivan, A. Rogers, D. Flynn, P. Smith, A. Mullane, and M. O' Malley, "Studying the maximum instantaneous non-synchronous generation in an island system-frequency stability challenges in Ireland," *IEEE Trans. Power Syst.*, vol. 29, no. 6, pp. 2943–2951, Nov. 2014.
[34] C. M. Affonso, W. Freitas, W. Xu, and L. C. P. da Silva, "Performance of ROCOF relays for embedded generation applications," *IEE Proc. Gener. Trans. Distrib.*, vol. 152, pp. 109–114, 2005.
[35] PPA Energy, "Rate of Change of Frequency (ROCOF) – Review of TSO and Generator Submissions," PPA Energy, Guildford, U.K., Tech. Rep. 13143, 2013.

Sotirios I. Nanou (M'12) received the Diploma in electrical and computer engineering, and the Ph.D. degree, both from the National Technical University of Athens, Zografou, Greece, in 2009 and 2016, respectively, where he is currently working as a Postdoctoral Researcher in the Laboratory of Electric Machines and Power Electronics. He worked for the Hellenic Electricity Distribution Network Operator (HEDNO S.A.), where he was engaged in power generation expansion planning studies for the Aegean Sea island systems. His research interests include the field of HVDC transmission based on VSCs, and grid code compatibility of HVDC systems and renewable energy stations. He is a member of the Technical Chamber of Greece.

Stavros A. Papathanassiou (S'93–M'98–SM'10) received the Diploma in electrical engineering and the Ph.D. degree both from the National Technical University of Athens (NTUA), Zografou, Greece, in 1991 and 1997, respectively. He worked for the Distribution Division, Public Power Corporation of Greece in power quality and distributed generation studies. In 2002 he became a member of the faculty in the Electric Power Division of NTUA, where he currently serves as Associate Professor. From 2009 to 2012, he was a member of the Board of Directors of the Hellenic TSO and Market Operator. His research interests include renewable energy technologies and the integration of DG to the grid. He is a member of CIGRE.